The Astrophysical Journal, 833:269 (6pp), 2016 December 20 doi:10.3847/1538-4357/833/2/269

COLLISIONAL DESTRUCTION OF FeC_n^- ($n = 1$ TO 4, 6) ANIONS OF ASTROPHYSICAL RELEVANCE

M. Nrisimhamurty[1], R. G. Mane[2], Roby Chacko[1], A. K. Gupta[2], P. C. Deshmukh[1,3], and G. Aravind[1]
[1] Indian Institute of Technology Madras, Chennai 600 036, India; garavind@iitm.ac.in
[2] Nuclear Physics Division, Bhabha Atomic Research Centre, Mumbai 400 085, India
[3] Indian Institute of Technology Tirupati, Tirupati 517 506, India
Received 2016 August 2; revised 2016 October 29; accepted 2016 November 2; published 2016 December 21

ABSTRACT

The stability of FeC^- against dissociation in an astrophysical environment was probed by the collisional excitation of FeC^-. Two anion resonances yielding Fe^- and C^- fragments were observed and studied through measurement of the kinetic energy released during fragmentation. The yield of Fe^- was found to be nearly 5.5 times more than that of C^- indicating the C^- fragment to be in the loosely bound (^2D) state. The possibility of avoided crossing leading to the observed fragment ion yield is also discussed. The dissociation of FeC_n^- ($n = 2$ to 4, 6) cluster anions predominantly resulted in the cleavage of Fe–C bond yielding only C_n^- fragments with similar energy release. The yield of C_n^- is discussed in the light of the observed abundances of HC_n in IRC+10216. The importance of rotational transitions pertaining to both the ground and excited-electronic states of these cluster anions is discussed.

Key words: astrochemistry – ISM: abundances – ISM: kinematics and dynamics – ISM: lines and bands – ISM: molecules – stars: kinematics and dynamics

1. INTRODUCTION

The detection of iron-containing molecules in the interstellar medium (ISM) has been elusive, even though the abundance of iron in space is not low. Although the depletion of iron is prevalent in the ISM its gas-phase concentration is significant. This motivated Merer et al. (1982) and Walmsley et al. (2002) to search for FeO in the ISM. The observation of ground-state rotational transitions enabled the detection of FeO toward Sagittarius B2 by Furuya et al. (2003). Recently, Zack et al. (2011) unambiguously identified a new interstellar molecule, FeCN, in the envelope of the carbon-rich asymptotic giant branch star, IRC+10216. Furthermore, nearly six carbon-containing anions were detected and the most prolific existence of these anions is also in the same carbon-rich star, IRC +10216. These discoveries are rather motivating in the search for anions of molecules containing both Fe and C, like FeC^-, in the ISM. The recent identification of C_{60}^+ in the ISM by Campbell et al. (2015) further motivates studies on iron–carbon clusters. It is important to note that although the search for neutral and cationic species in the ISM has been undertaken for decades, only recently has a rigorous search for anions been carried out. The earlier prediction of Herbst (1981) and the recent detections of CN^- (Agúndez et al. 2010), C_3N^- (Thaddeus et al. 2008), C_4H^- (Cernicharo et al. 2007; Gupta et al. 2007), C_6H^- (McCarthy et al. 2006; Sakai et al. 2007), and C_8H^- (Gupta et al. 2007; Kawaguchi et al. 2007; Remijan et al. 2007) have confirmed the abundance of anions in the interstellar space. CN^-, C_3N^-, C_4H^-, and C_5N^- have also been identified by Vuitton et al. (2009) in Titan's atmosphere. Furthermore, anions are involved in a variety of processes like radiative attachment, dissociative electron attachment (DEA), photodetachment, associative detachment, etc., which determine the constituents of ISM. Studies on the anionic state of these molecules will also throw light on their neutral state and hence probing them is necessary in the search for their existence in the ISM. Although there are some exceptions like TaC^- (Aravind et al. 2015), anions have at most one bound electronic state with the excited states embedded in the detachment continuum. These excited anion states are important to understand their stability (Kumar et al. 2013) and the reactions they are involved in the astrophysical environment (Prabhudesai et al. 2005).

As mentioned earlier, the observations of FeCN and carbon-containing anions in IRC+10216 motivates our present work on FeC_n^- ($n = 1$ to 4, 6). Ab initio calculations for the ground states of FeC, FeC^+, and FeC^- (Tzeli & Mavridis 2010), structure and binding energy calculations for FeC_n ($n = 1$ to 4) (Noya et al. 2003; Hendrickx & Clima 2004), and FeC_2^- and FeC_3^- (Hendrickx & Clima 2004) have been reported. Redondo et al. (2009) calculated electronic and geometrical structures of the ground and excited states for FeC_n^- ($n = 1$ to 8). UV spectra of iron-doped carbon clusters FeC_n ($n = 3$ to 6) (Steglich et al. 2014) and anion photoelectron spectroscopy on FeC_2^- (Fan & Wang 1994; Li & Wang 1999) and FeC_n^- ($n = 3$, 4) (Fan et al. 1995; Wang & Li 2000) are the only experimental studies on FeC_n. The bonding and structural properties of FeC_2^- (Li & Wang 1999) and FeC_3^- (Wang & Li 2000) were probed experimentally. To the best of our knowledge, there are no previous theoretical or experimental studies on the FeC^- anion resonances.

1.1. Significance of the Present Work

The electron affinities of FeC_n ($n = 1$ to 4, 6) clusters indicate that they can form stable negative ions (Fan & Wang 1994, Fan et al. 1995). While the rotational transitions are important to probe the existence of neutral molecules in the ISM, the study of excited states (resonances) of anions is of paramount importance in their search and particularly in understanding the reactions they undergo. These anion states are distinguished as shape, core-excited shape, nuclear-excited Feshbach, and electron-excited Feshbach resonances. The lifetime of these anion resonances can vary from microseconds to a few femtoseconds, depending on whether they lie energetically above or below the neutral electronic state. Anion resonances could eventually detach an electron or dissociate, and hence could also explain the concentration of the particular anionic fragment in the ISM. It is a formidable task to theoretically probe the anion resonances due to high electron

correlations in these states. In the present work, we study the collisional destruction of FeC_n^- ($n = 1$ to 4, 6) anions, which is important to understand their stability in the ISM. In the ISM, these resonances could also be accessed by UV absorption of ground-electronic states of FeC_n^- ($n = 1$ to 4, 6) anions. Our results on FeC_n^- ($n = 1$ to 4, 6) anions are important to glean their structures. We observe two anion resonances for FeC^- leading to Fe^- and C^- fragments, with the yield for the former being higher. FeC_n^- ($n = 2$ to 4, 6) anions are found to fragment, yielding C_n^- ($n = 2$ to 4, 6) anions indicating the intrinsic stability of C_n^- ($n = 2$ to 4, 6) anions, which are proposed ISM candidates. We believe that our experimental results should aid in the search for iron–carbon clusters in the ISM.

2. EXPERIMENTAL SECTION

The experimental setup employed is described in detail elsewhere (Gupta & Krishnamurthy 2003). Briefly, a Cs-sputter anion source with the cathode sample made of a mixture of iron and graphite was sputtered with 1 keV Cs ions. The anions thus formed were accelerated to 15 keV and a double focusing 90° magnet was used to mass separate the ions of interest. Although the FeC^- was produced with high intensity, it was rather nontrivial to produce the FeC_n^- cluster anions. The mass-selected anions were then collided with Ar gas in the collision cell at a chamber pressure of 2×10^{-6} Torr, where the base pressure is 2×10^{-7} Torr. Anions scattered in the forward direction (angular resolution of $\pm 0.^{\circ}01$) were energy analyzed using an electrostatic parallel plate analyzer. A channeltron together with the pulse counting electronics are used to detect the ions. The energy analysis yields the kinetic energy distribution of the anionic fragments in the lab frame.

3. RESULTS AND DISCUSSION

The projectile anion is collisionally excited to the anion resonance state, which eventually fragments into anionic and neutral fragments. Autodetachment of the anion resonance is also a competing process. During fragmentation, the energy released in the center-of-mass frame (CM frame) is shared between the fragments in the inverse ratio of their masses. We employ translational energy spectrometry, which allows amplification of low kinetic energies released in the CM frame. Furthermore, since our detection is confined to anion fragments scattered along the forward angles, only large-impact parameter collisions are probed and the momentum imparted to the target atom will be negligible. Most importantly, fragments formed from scattering at large-impact parameters predominantly results in electronic excitation rather than conversion of the collisional energy into vibrational energy (Gupta & Krishnamurthy 2003). The measured kinetic energy distributions for anionic fragments are then employed to deduce the shape of the potential-energy function of the anion resonance.

Figure 1 shows lab-frame kinetic energy release distribution ($KERD_{lab}$) for the fragment ions formed post collision-induced dissociation (CID). The striking feature of the result is the formation of both Fe^- and C^- fragments from two different fragmentation channels activated by the collisional interaction. The spread in $KERD_{lab}$ for the parent anion (not shown) about its centroid value ($E_p = 15$ keV) is due to the spread in their energy during formation and the instrumental resolution. The parent ion $KERD_{lab}$ profile is employed to deconvolute the

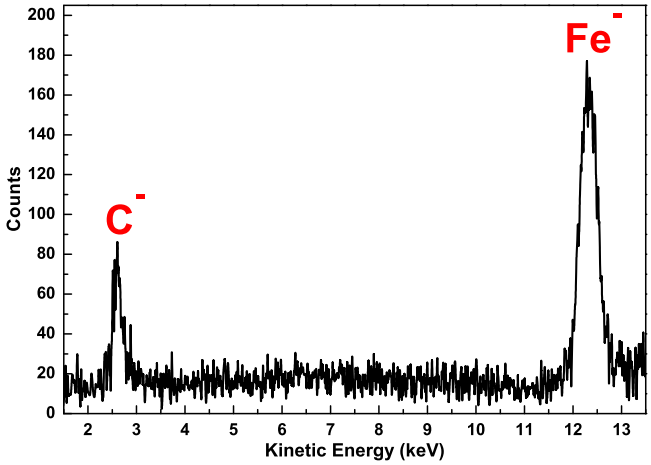

Figure 1. Daughter-ion peaks recorded for the CID of FeC^- anion.

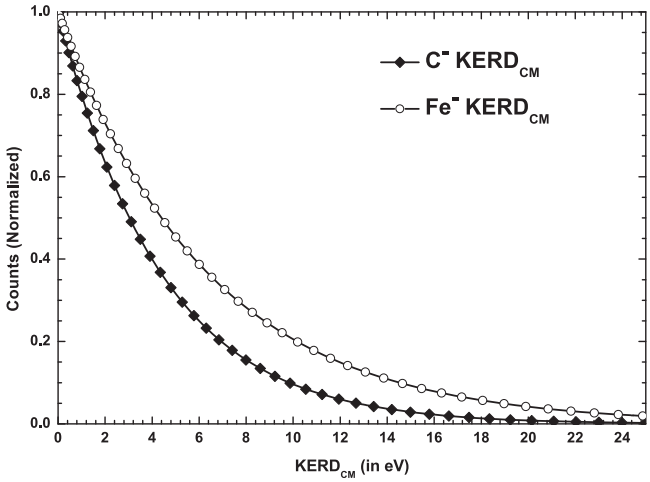

Figure 2. Normalized kinetic energy distribution in the CM frame for Fe^- and C^- daughter anions.

daughter-ion spectra to yield the actual $KERD_{lab}$ for the fragment anions. The spread in the deconvoluted daughter peaks corresponds to the energy released in the CM frame ($KERD_{CM}$) during the dissociation. The total KE released in the CM frame, E_{CM}, is related to the lab-frame kinetic energy, E_1, of the fragment ion m_1 as

$$E_1 = \frac{m_1}{M}E_p' + \frac{2\sqrt{E_{CM}E_p' m_1 m_2}}{M} + \frac{m_2}{M}E_{CM} \quad (1)$$

$$E_p' = (E_p - E_{CM} - Q) \quad (2)$$

where M and m_2 are masses of the parent ion and the neutral fragment, respectively, and Q is the total internal excitation energy for both the projectile and the target. We observed a shift in the observed energy peaks for the anions corresponding to a total internal excitation of about 20 eV.

Figure 2 shows the $KERD_{CM}$ for the two fragmentation pathways, which lead to different fragment ions. $KERD_{CM}$ depends on the shape of the excited-state potential-energy curve and hence the results clearly indicate that two different negative-ion resonances are accessed upon collisional excitation.

We performed potential-energy surface calculation for the ground-electronic state of the FeC^- anion using the

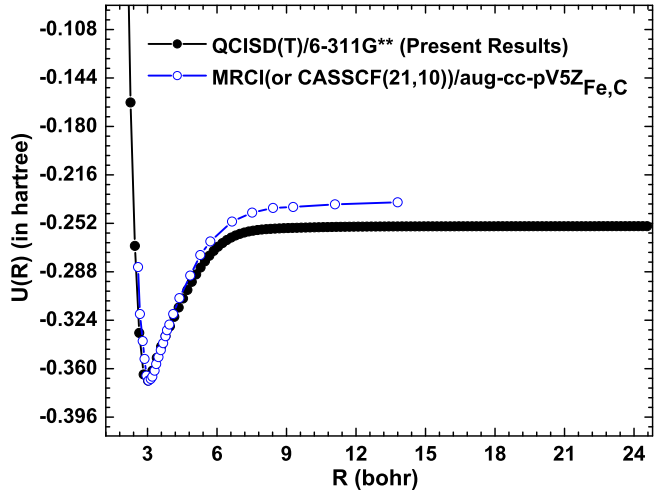

Figure 3. Potential-energy curves, energy-shifted for comparison, for the ground-electronic state of the FeC^- anion.

6-311G(d,p) basis set and QCISD(T) methodology with Gaussian 09 (Frisch et al. 2009). The ground-electronic state of FeC^- was found to be $^2\Delta$. In Figure 3, our calculated potential-energy surface is compared with that of a recent calculation by Tzeli & Mavridis (2010), who employed MRCI calculations. Apart from the potential-energy surface, we also compare our results on equilibrium bond distance (r_e) and bond-dissociation energy (D_e) for the ground state of FeC^- in Table 1. Transitions to the negative-ion resonance occur from the vibrational states of the ground-electronic state of the anion. The probability for the transition to the excited state is given by the overlap integral for the wavefunctions of the initial and the final states. These vibrational wavefunctions for the ground-electronic state were calculated using LEVEL (Le Roy 2015). LEVEL can be employed to compute ro-vibrational eigenvalues and eigenfunctions for smoothly varying one-dimensional or radial potential-energy functions using the semiclassical WKB method. Considering a vibrational temperature of about 1000 K for the ions produced in the source, we have included excited vibrational levels of the ground-electronic state with appropriate weight factors. A delta function at the classical turning point is taken as the wavefunction for the excited state. We employ the reflection method to deduce the excited potential-energy state that leads to the observed fragment ions (Gupta & Krishnamurthy 2003). $KERD_{CM}$ is simulated by reflecting the nuclear wavepacket on a Lennard–Jones (LJ) potential given by

$$V(r) = \frac{A}{r^{12}} - \frac{B}{r^6}. \quad (3)$$

The parameters of this potential were determined by fitting the simulated $KERD_{CM}$ with the observed $KERD_{CM}$.

Figures 4 and 5 shows the fit of the simulated $KERD_{CM}$ with the observed $KERD_{CM}$ for both the anions. The fitting parameters A and B of the LJ potential were $A = 3659\,\text{eV Å}^{12}$, $B = 150\,\text{eV Å}^6$ for the state yielding C^-, and $A = 5391\,\text{eV Å}^{12}$, $B = 205\,\text{eV Å}^6$ for the state yielding Fe^-.

Figure 6 shows the deduced excited-state potential-energy curves along with the ground-electronic state. The yield of the Fe^- anion is nearly 5.5 times more than that of the C^- anion, in spite of larger electron affinity for the C^- anion. This implies that the C^- fragment is in ^{2}D state, whose binding energy is

Table 1
Comparison of the Present Results with the Tzeli & Mavridis (2010) Calculations for Absolute Energy E(hartree), Bond Length r_e (Å), and Bond-dissociation Energy D_e (kcal mol^{-1}) of the Ground State of FeC^-

Methodology	Absolute Energy ($-E$) (in hartree)	Bond length (r_e) (in Å)	Bond Dissociation Energy (D_e) (in kcal mol^{-1})
QCISD(T)[a]	1300.36942	1.574	72.11
MRCI[b]	1300.587387	1.6132	84.28
C-MRCI[b]	1300.987066	1.6079	86.62
C-MRCI+DKH8[b]	1309.921685	1.6036	78.32
C-MRCI +DKH8+Q[b]	1310.00353	1.5998	84.39
QCISD[a]	1300.08797	1.575	61.68

Notes. QCISD(T)-Quadratic configuration interaction (CI) with single-, double-, and triple-excitations added perturbatively; QCISD-Quadratic CI calculation, including single and double substitutions; In the present work, we have used the 6-311G(d,p) basis set (Hay 1977) for all the calculations using Gaussian 09 (Frisch et al. 2009).
MRCI-Multireference configuration interaction. Here, C-MRCI indicates that ^{56}Fe $3s^23p^6$ subvalence electrons have been included in the CI whereas +Q and +DKH8 refer to the multireference Davidson correction for unlinked clusters and to 8th-order Douglas–Kroll–Hess scalar relativistic corrections, respectively. The basis sets employed in these MRCI calculations by Tzeli & Mavridis (2010) are aug-cc-pV5Z(-DK)$_{Fe,C}$ (Dunning 1989; Woon & Dunning 1995) and aug-cc-pwCV5Z(-DK)$_{Fe,C}$ (Balabanov & Peterson 2005).
[a] Present Results.
[b] Reported by Tzeli & Mavridis (2010).

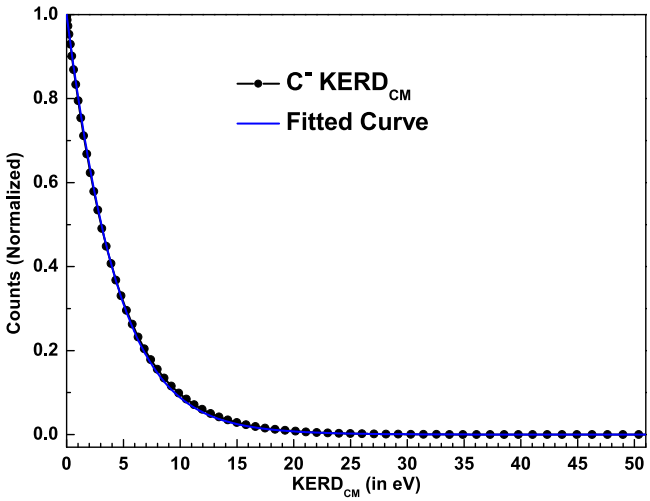

Figure 4. Experimentally deduced kinetic energy release distribution in the CM frame ($KERD_{CM}$) for the C^- anion is shown along with a fit to it, considering an LJ potential (see the text).

known to be about 33 meV (Scheer et al. 1998). Energetically, the asymptote of the excited state, which leads to the C^- daughter would also then lie above the asymptote of the excited state, which leads to Fe^-. The larger binding energy of $Fe^-(^4F)$ (Leopold & Lineberger 1986) when compared to $C^-(^2D)$ could be the reason for the lower yield of C^-. The symmetries of these excited resonances are best studied through the measurement of the angular distribution of fragments following DEA (Ómarsson et al. 2014). If the symmetries of these two resonance states are the same, being a diatomic molecule, there could be an avoided crossing. The transition of FeC^- from a resonance state with C^- at its

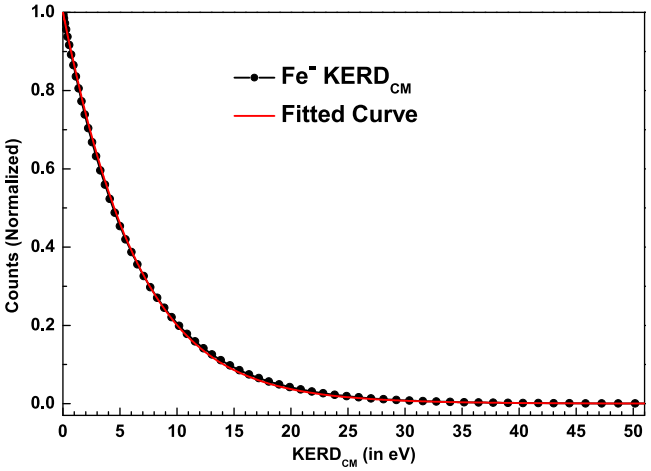

Figure 5. Experimentally deduced kinetic energy release distribution in the CM frame ($KERD_{CM}$) for the Fe^- anion is shown along with a fit to it, considering an LJ potential (see the text).

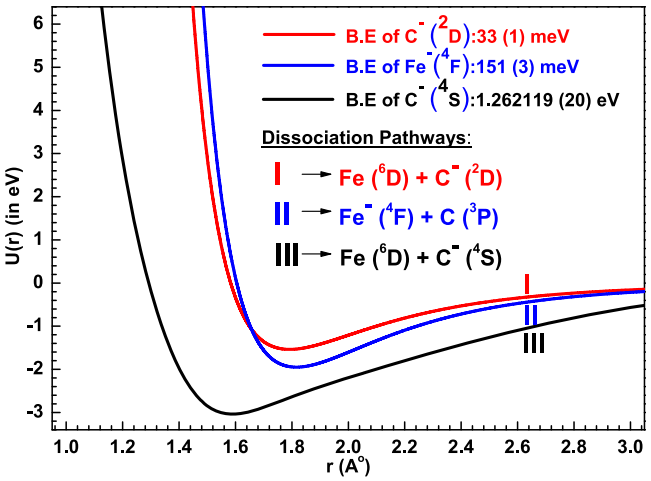

Figure 6. Deduced excited-electronic states and the computed energy curve for the ground-electronic state of the FeC^- anion.

asymptotic limit to the other resonance with Fe^- at its asymptotic limit could occur at such an avoided crossing. This could also be the reason for the lower C^- yield. Under our collision conditions, the presence of the target gas might lead to different symmetries for the two FeC^- resonances, resulting in the strong coupling of these two channels. As mentioned earlier, excited-electronic states of the anions are mostly embedded in the detachment continuum. However, we had recently reported a stable excited anion state for another transition-metal carbide anion TaC^- (Aravind et al. 2015). To the best of our knowledge, there is no theoretical calculation available on the excited-electronic potential-energy surfaces for FeC^- and our results stress the necessity to perform the same. The presence of a large number of closely lying electronic states for FeC (Tzeli & Mavridis 2010) implies the plausible high density of excited states for FeC^-, which could be challenging for theoretical computations.

It is important to note that anion resonances can be accessed by electron attachment to neutral states as in DEA experiments and through photo-excitation of the ground anion state. These two methods and our present approach are complementary, since different regions of the excited potential-energy states will be accessed by these techniques due to the differing

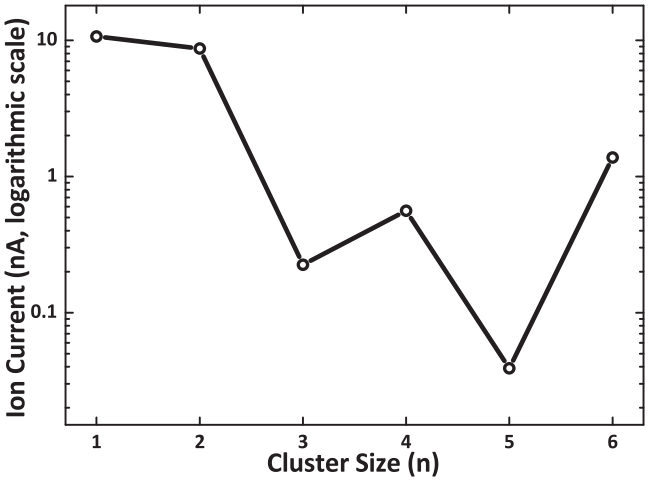

Figure 7. Yield of the FeC_n^- ($n = 1$ to 6) clusters in the sputter source.

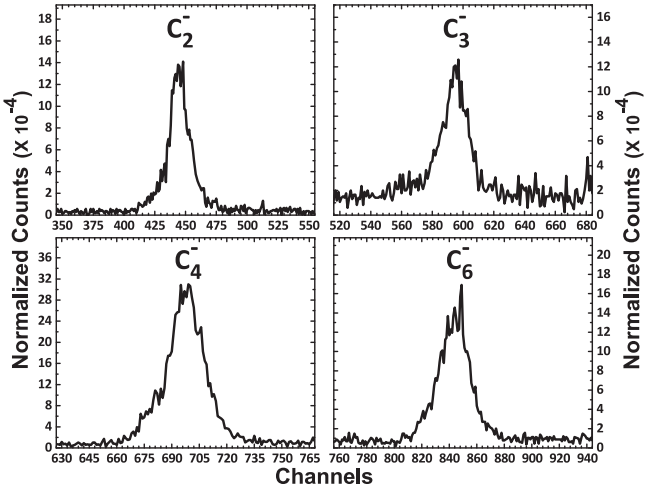

Figure 8. Daughter cluster-ion peaks that are formed during the CID of the FeC_n^-($n = 2$ to 4, 6) clusters. Only one daughter-ion peak corresponding to the Fe–C bond cleavage is observed.

geometries of the initial states. Accessing different regions of the complex excited potential-energy surface could lead to different fragmentation channels. To the best of our knowledge, the other two techniques are not yet employed on this anion, which is of astrophysical relevance.

3.1. Dissociation of FeC_n^- ($n = 2$ to 4, 6) Clusters

It is interesting to compare the relative yields of the FeC_n^- ($n = 1$ to 6) anions from the sputter source. Electron affinities for the C_n^- clusters have oscillatory behavior (Arnold et al. 1991), where clusters with even n have larger electron affinity than their neighbors with odd n. The yield of FeC_n^- ($n = 1$ to 6), as shown in Figure 7, nearly shows such a behavior.

Figure 8 shows the fragment anions observed for the FeC_n^- ($n = 2$ to 4, 6) clusters. Unlike the case of FeC^-, C_n^- (n = 2 to 4,6) were the only fragment ions observed, indicating that other fragmentation channels are much weaker. Low yield of the parent anions of higher clusters from the sputter source could also be the reason for not observing other weak fragmentation channels. The dissociation dynamics for FeC^- is evidently distinct from that for the FeC_n^- ($n = 2$ to 4, 6) clusters with its dominant Fe^- channel. In the higher anionic clusters, the fact that the C–C bond is much stronger than the Fe–C bond,

Table 2
Yield of C_n^- Fragments Upon Collisional Excitation of FeC_n^-

Parent Ion (FeC_n^-)	Fractional Yield of Daughter-ion (C_n^-) x 10^{-4}
FeC_2^-	9.52
FeC_3^-	9.61
FeC_4^-	37.95
FeC_6^-	16.83

determines the dominant C_n^- ($n = 2$ to 4, 6) fragment channel. Structural calculations on the anion resonances of these clusters needs to be performed to understand if possibly the linear structure in the resonance state leads to the observed dominant channel in addition to any weak fragmentation channel. It is known from both experimental and theoretical studies that the structure of the neutral ground state of these clusters is not linear (Hendrickx & Clima 2004). Photoelectron spectroscopic results for FeC_4^- (Fan et al. 1995) had indicated a drastic change in the geometry of the anion when compared to the neutral ground state.

3.2. Astrophysical Relevance of the Present Results

Dissociation dynamics of these iron–carbon clusters may play an important role in the formation of large interstellar dust. Table 2 shows the yield of C_n^- upon CID of the FeC_n^- anions. The formation of C_n^- as a dominant fragment implies the intrinsic stability of these cluster anions in the ISM.

Barckholtz et al. (2001) experimentally showed that C_n^- is almost unreactive toward H_2. However, with atomic hydrogen they undergo either associative electron-detachment ($C_n^- + H \longrightarrow HC_n + e^-$) or form an associative product anion ($C_n^- + H \longrightarrow HC_n^-$), with the former being the exclusive pathway for $n \leqslant 6$ (Blanksby et al. 2001). Cernicharo et al. (2007) observed the abundance of HC_4 to be about 45 times higher than that of HC_6 in IRC +10216. In our experiment, the ratio $[C_4^-]/[C_6^-]$ is about 2.3 and from the results of Barckholtz et al. (2001), it can be asserted that the $C_{n=4,6}^-$ fragments from $FeC_{n=4,6}^-$, could undergo associative electron-detachment to yield $HC_{n=4,6}$, in the H-atom abundant regions of the ISM. Electron-detachment (collision/photon induced) of C_n^- will be another competing pathway yielding C_n, which is abundant in ISM (Cordiner & Millar 2009). Fe^-, a dominant fragment from the CID of FeC^-, could undergo associative electron-detachment with CN and yield FeCN in the ISM (Zack et al. 2011).

It is important to note that the adiabatic electron affinity for FeC (1.15 eV by Tzeli & Mavridis 2010) is lower than the calculated dissociation energy of the anion. Thus, even the higher vibrational levels of the ground-electronic state ($^2\Delta$) of FeC^- are autodetaching states. Furthermore, any possible excited-electronic state of FeC^-, which is stable against electron-detachment, should lie very close to the ground state. Such stable excited-electronic states have been experimentally observed for many transition-metal carbide anions such as WC^- (Rothgeb et al. 2008), MoC^- (Liu et al. 2015), TaC^- (Aravind et al. 2015), and FeC_2^- (Li & Wang 1999). Hence, the rotational transitions pertaining to the ground as well as the stable excited-electronic states of FeC_n^- should be searched in the Diffused Interstellar Bands. To the best of our knowledge, rotational spectroscopy on FeC_n^- is yet to be performed. Furthermore, although it is believed that atomic iron is heavily depleted in the ISM (Steglich et al. 2014), the higher yield of Fe^- than C^- in the CID of FeC^- correlates with the observed abundance of Fe in the IRC +10216 (Mauron & Huggins 2010). Current results on anionic clusters should aid in understanding the formation of condensed interstellar dust (Herbst 2001).

4. CONCLUSIONS

Collision-induced dissociation of FeC_n^- ($n = 1$ to 4, 6) clusters was carried out and two anion resonances for FeC^- were observed for the first time. These two anion resonances yield two different fragments, namely, Fe^- and C^-. The potential-energy surface for the FeC^- anion resonances were deduced from the measured kinetic energy released during fragmentation in the lab frame. A strikingly higher yield of Fe^- indicates that the C^- fragment is in the loosely bound ^2D state. The symmetries of the observed anion resonances could be the same, leading to an avoided crossing. Transition across this avoided crossing could lead to the observed higher yield of Fe^- fragments. The possibility for the coupling of these two resonances in the presence of the target gas is also discussed. A Velocity Map Imaging study on DEA in FeC should throw light on the symmetries of the anion resonances, and the present results stress the requirement of the same. Considering the high density of electronic states in FeC, the theoretical calculation for the corresponding anion could be a formidable task and our results should guide such computations. The present work stresses the need for theoretical calculations on the FeC^- anion resonances, particularly to study transition through an avoided crossing, resulting in lower yield for C^-. Fe^-, which is the dominant fragment from FeC^-, and could be the precursor for FeCN in the ISM. C_n^- ($n = 2$ to 4, 6) is the dominant fragment from FeC_n^- ($n = 2$ to 4, 6) and its yield is compared with the abundance of HC_n in IRC+10216. It is important to search for rotational transitions pertaining to both the ground and excited-electronic states of FeC_n^- in their detection in IRC +10216. The present results are important in understanding the stability of the FeC_n^- ($n = 1$ to 4, 6) clusters in an astrophysical environment and also the chemical reactions in which they participate.

We thank Y. Sajeev for stimulating discussions on the dissociation dynamics of FeC^-. This work was partially funded by the Board of Research in Nuclear Science, Department of Atomic Energy, India.

REFERENCES

Agúndez, M., Cernicharo, J., Guélin, M., et al. 2010, A&A, 517, L2
Aravind, G., Nrisimhamurty, M., Mane, R. G., Gupta, A. K., & Krishnakumar, E. 2015, PhRvA, 92, 042503
Arnold, D. W., Bradforth, S. E., Kitsopoulos, T. N., & Neumark, D. M. 1991, JChPh, 95, 8753
Balabanov, N. B., & Peterson, K. A. 2005, JChPh, 123, 064107
Barckholtz, C., Snow, T. P., & Bierbaum, V. M. 2001, ApJL, 547, L171
Blanksby, S. J., McAnoy, A. M., Dua, S., & Bowie, J. H. 2001, MNRAS, 328, 89
Campbell, E. K., Holz, M., Gerlich, D., & Maier, J. P. 2015, Natur, 523, 322
Cernicharo, J., Guélin, M., Agúndez, M., et al. 2007, A&A, 467, L37
Cernicharo, J., Guélin, M., Agúndez, M., McCarthy, M. C., & Thaddeus, P. 2008, ApJL, 688, L83
Cordiner, M. A., & Millar, T. J. 2009, ApJ, 697, 68

Dunning, T. H., Jr. 1989, JChPh, 90, 1007
Fan, J., Lou, L., & Wang, L.-S. 1995, JChPh, 102, 2701
Fan, J., & Wang, L.-S. 1994, JPhCh, 98, 11814
Frisch, M. J., Trucks, G. W., Schlegel, H. B., et al. 2009, Gaussian 09, Revision E.01 (Wallingford, CT: Gaussian, Inc.)
Furuya, R. S., Walmsley, C. M., Nakanishi, K., Schilke, P., & Bachiller, R. 2003, A&A, 409, L21
Gupta, A. K., & Krishnamurthy, M. 2003, PhRvA, 67, 023201
Gupta, H., Brünken, S., Tamassia, F., et al. 2007, ApJL, 655, L57
Hay, P. J. 1977, JChPh, 66, 4377
Hendrickx, M. F. A., & Clima, S. 2004, CPL, 388, 290
Herbst, E. 1981, Natur, 289, 656
Herbst, E. 2001, Chem. Sov. Rev., 30, 168
Kawaguchi, K., Fujimori, R., Aimi, S., et al. 2007, PASJ, 59, L47
Kumar, S. S., Hauser, D., Jindra, R., et al. 2013, ApJ, 25, 776
Leopold, D. G., & Lineberger, W. C. 1986, JChPh, 85, 51
Le Roy, R. J. 2015, LEVEL 8.2: A Computer Program for Solving the Radial Schrödinger Equation for Bound and Quasibound Levels, Chemical Physics Research Rep. CP-668 (Univ. Waterloo), http://scienide2.uwaterloo.ca/rleroy/level/
Li, X., & Wang, L. S. 1999, JChPh, 111, 8389
Liu, Q.-Y., Hu, L., Li, Z.-Y., et al. 2015, JChPh, 142, 164301
Mauron, N., & Huggins, P. J. 2010, A&A, 513, A31
McCarthy, M. C., Gottlieb, C. A., Gupta, H., & Thaddeus, P. 2006, ApJL, 652, L141
Merer, A. J., Walmsley, C. M., & Churchwell, E. 1982, ApJ, 256, 151
Noya, E. G., Longo, R. C., & Gallego, L. J. 2003, JChPh, 119, 11130
Ómarsson, F. H., Mason, N. J., Krishnakumar, E., & Ingólfsson, O. 2014, Angew. Chem. Int. ed., 53, 12051
Prabhudesai, V. S., Kelkar, A. H., Nandi, D., & Krishnakumar, E. 2005, PhRvL, 95, 143202
Redondo, P., Largo, L., & Barrientos, C. 2009, CP, 364, 1
Remijan, A. J., Hollis, J. M., Lovas, F. J., et al. 2007, ApJL, 664, L47
Rothgeb, D., Hossain, E., & Jarrold, C. C. 2008, JChPh, 129, 114304
Sakai, N., Sakai, T., Osamura, Y., & Yamamoto, S. 2007, ApJL, 667, L65
Scheer, M., Bilodeau, R. C., Brodie, C. A., & Haugen, H. K. 1998, PhRvA, 58, 2844
Steglich, M., Chen, X., Johnson, A., & Maier, J. P. 2014, IJMSp, 365, 351
Thaddeus, P., Gottlieb, C. A., Gupta, H., et al. 2008, ApJ, 677, 1132
Tzeli, D., & Mavridis, A. 2010, JChPh, 132, 194312
Vuitton, V., Lavvas, P., Yelle, R. V., et al. 2009, P&SS, 57, 1558
Walmsley, C. M., Bachiller, R., Pineau des Forêts, G., & Schilke, P. 2002, ApJL, 566, L109
Wang, L. S., & Li, X. 2000, JChPh, 112, 3602
Woon, D. E., & Dunning, T. H., Jr. 1995, JChPh, 103, 4572
Zack, L. N., Halfen, D. T., & Ziurys, L. M. 2011, ApJL, 733, L36